The Lipid/Protein Interface as Xenobiotic Target Site

KINETIC ANALYSIS OF THE NICOTINIC ACETYLCHOLINE RECEPTOR*

Received for publication, June 5, 2001, and in revised form, August 6, 2001 Published, JBC Papers in Press, August 6, 2001, DOI 10.1074/jbc.M105136200

Sebastian Walcher[‡], Joachim Altschuh[‡], and Heinrich Sandermann, Jr.[§]¶

From the ‡Institute of Biomathematics and Biometry and the §Institute of Biochemical Plant Pathology, GSF-National Research Center for Environment and Health, Ingolstädter Landstraβe 1, D-85764 Neuherberg, Germany

Membrane proteins are known to be solvated and functionally activated by a fixed number of lipid molecules whose multiple binding can be described by Adairtype binding equations. Lipophilic xenobiotics such as general anesthetics may act by competitive displacement of protein-bound lipids. A kinetic equation is now presented for various binding stoichiometries of lipid and xenobiotic, and microscopic binding constants of anesthetics and organic solvents are derived from two independent assay systems for the enhancement of agonist binding to the nicotinic acetylcholine receptor. These constants lead to the first available free energy estimate (-6.4 kcal/mol) for the binding of membrane lipid to an integral membrane protein.

The target sites of general anesthetics are still controversial. Hydrophobic protein regions are now emphasized more strongly than membrane lipids, the lipid/protein interface being a much less studied candidate target site (1, 2). Most functional membrane proteins have an obligatory lipid requirement, and Adair-type equations have been developed for the analysis of lipid activation on multiple protein binding sites analogous to hemoglobin and soluble allosteric enzymes (3, 4). This approach has led to the following main results. (i) The characteristic positive kinetic cooperativity of lipid-dependent enzymes could be reconciled with the lack of cooperativity detected by electron spin resonance spectroscopy (3, 4). (ii) A truly allosteric lipid activator (phosphatidylcholine) was identified for the first time in the case of the mitochondrial β -hydroxybutyrate dehydrogenase (5, 6), as recently confirmed with improved techniques (7). (iii) The postulated highly allosteric interaction of multiple phosphatidylserine molecules with protein kinase C (8, 9) was attributed to a kinetic artifact (10), as confirmed more recently (11).

The present article introduces a new general kinetic equation and applies it to a well characterized gated channel protein for anesthesia research, the *Torpedo* nicotinic acetylcholine receptor (nAChR). Many physical and biochemical techniques have been applied to this membrane protein to elucidate target sites of general anesthetics, but multiple mechanisms appeared

to exist, and results have remained complicated (2). Progress seems to depend on the further development of techniques. The multiple-site kinetic approach developed in this article adds to the experimental repertoire by allowing an assessment of the lipid/protein interface as an anesthetic target site.

EXPERIMENTAL PROCEDURES

The experimental data were obtained with highly purified nAChRrich membranes isolated from electroplaques of Torpedo nobiliana (12, 13). About 200 lipid molecules per receptor molecule are known to be present in such membranes (14). A data set for the enhanced binding of [3H]acetylcholine to ~30 nm nAChR by ethanol, 1-hexanol, ether, and methoxyflurane, respectively, was adopted from Ref. 12 (Fig. 1 therein). The lower and upper plateau values of enhancement were set as 0 and 100%, respectively. An independent assay to determine enhanced agonist binding by 1-butanol and isoflurane, respectively, employed the fluorescent acetylcholine analogue, [1-(5-dimethylaminonaphthalene)sulfonamido]-n-hexanoic acid β -(N-trimethylammonium bromide) ethyl ester (Dns-C₆-Cho), using 200 nm nAChR (13). The data points of Ref. 13 (Fig. 6a therein) were used, again setting the lower and upper plateau values as 0 and 100%, respectively. Analogous to extensive previous work (4, 6, 15) lipid and xenobiotic concentrations are expressed as the number of lipid or xenobiotic molecules per nAChR molecule. Under the conditions of Ref. 12. 1 mm xenobiotic corresponded to 33,000 xenobiotic molecules per nAChR molecule. Under the conditions of Ref. 13, 1 mm xenobiotic corresponded to 5,000 xenobiotic molecules per nAChR molecule. The total lipid concentration was always set as 200 molecules per nAChR molecule (14). Numerical computations and simulations were performed with the MATHEMATICA 3.0 software package.

RESULTS AND DISCUSSION

Mathematical Model—The present mathematical formalism is an extension of the Adair-type formalism for lipid activation (3), which had already been extended to the inhibition of lipid-dependent membrane proteins by lipophilic xenobiotics assuming a 1:1 exchange between lipid and xenobiotic (15–17). The lipid/protein interface is thought to consist of a lipid ring surrounding a membrane protein, where a fixed number n of lipid binding sites are present. This number has in many cases been determined by electron spin resonance spectroscopy. According to the general model (3), an integer number a of vacant sites is tolerated so that the protein is fully functional if at least (n-a) sites are occupied by lipid molecules and inactive with less than (n-a) lipid molecules. When xenobiotic molecules also bind to these sites, they contribute to inactivity or to new catalytic properties of the protein.

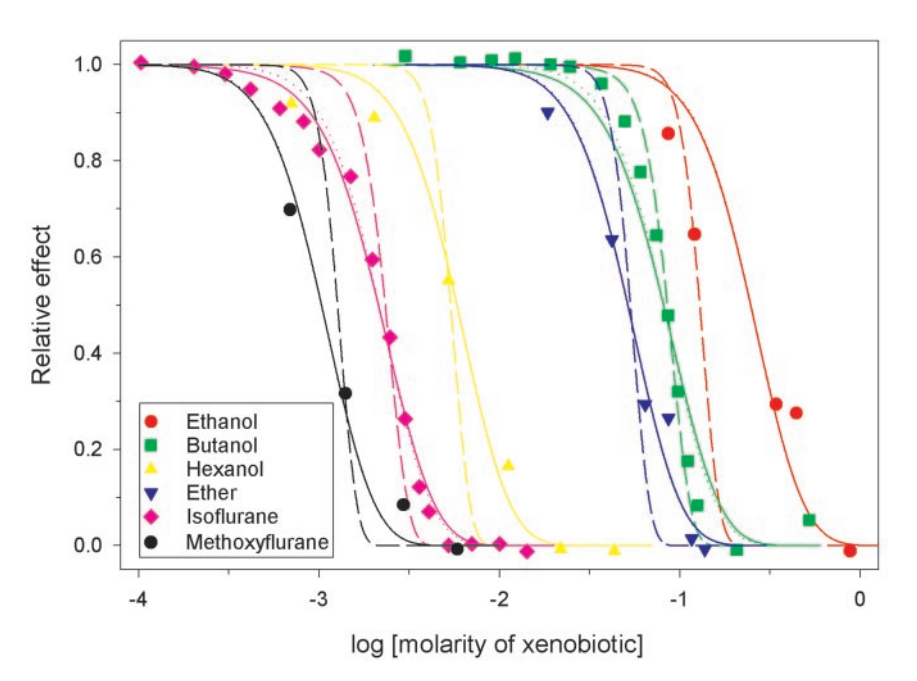
The relative proportion r of functional protein is of central interest, and we give a closed form expression for r. We assume (as is customary) mass-action kinetics and microscopic reversibility for the reactions, and moreover we assume that all microscopic binding constants are equal and that binding is noncooperative. We include the possibility of different stoichiometries between lipid and inhibitor; thus we allow one lipid binding site to be occupied by up to q inhibitor molecules. This approach takes into account the fact that the sizes of the

^{*} This work was supported by the Bayerisches Staatsministerium für Landesentwicklung und Umweltfragen. The costs of publication of this article were defrayed in part by the payment of page charges. This article must therefore be hereby marked "advertisement" in accordance with 18 U.S.C. Section 1734 solely to indicate this fact.

[¶] To whom correspondence should be addressed: GSF - National Research Center for Environment and Health, Institute of Biochemical Plant Pathology, Ingolstädter Landstraße 1, D-85764 Neuherberg, Germany. Tel.: 49-89-3187-2285; Fax: 49-89-3187-3383; E-mail: sandermann@gsf.de.

 $^{^1}$ The abbreviations used are: nAChR, nicotinic acetylcholine receptor; Dns-C₆-Cho, [1-(5-dimethylaminonaphthalene)sulfonamido]-n-hexanoic acid β -(N-trimethylammonium bromide) ethyl ester.

FIG. 1. Regression curves for enhanced agonist binding induced by xenobiotics. Enhancement (%) is plotted versus log (molar xenobiotic concentration). Regression analysis was based on 1:1 or 1:3 stoichiometries between lipid and xenobiotic binding as described under "Results and Discussion." Equations 1 and 2 were applied for the 1:1 scenario (full), 1:3 scenario 1 (dotted), and 1:3 scenario 2 (broken).



molecules in question are markedly different. Because little is known about the precise binding kinetics near the lipid ring, variations of and alternatives to the standard model have to be considered. The model and the underlying assumptions are presented in greater detail in the "Appendix."

We consider two scenarios. In the first scenario, a lipid can no longer bind to a site occupied by q xenobiotic molecules but can bind to all other sites. In other words, only receptor sites completely filled to stoichiometric number q by xenobiotic molecules are not available for lipids. In the contrasting second scenario, a lipid can only bind to sites not occupied by any xenobiotic molecules.

Introducing the lipid concentration [L], the inhibitor concentration [I], and the corresponding microscopic dissociation constants K_L and K_I , respectively, we abbreviate $x = [L]/K_L$ and $y = [I]/K_I$. Then the general expression for the relative proportion r in the first scenario is given by Equation 1. (Also, see "Appendix.").

$$r = \frac{\sum_{d=0}^{a} \binom{n}{d} y^{qd} \cdot (1 + y + \dots + y^{q-1})^{n-d} \cdot \sum_{l=n-a}^{n-d} \binom{n-d}{l} x^{l}}{((1+x) \cdot (1+y+\dots + y^{q-1}) + y^{q})^{n}}$$
(Eq. 1)

In the second scenario, one obtains the general expression shown in Equation 2. (Also, see "Appendix.")

$$r = \frac{\sum_{d=0}^{a} \binom{n}{d} \cdot (y + \dots + y^q)^d \cdot \sum_{l=n-a}^{n-d} \binom{n-d}{l} \cdot x^l}{(1 + x + y + \dots + y^q)^n}$$
 (Eq. 2)

Applied biochemically, r corresponds to relative effect or to fraction activity, maximum activity being r = 1.0.

Enhancement of Agonist Binding—The above Equations 1 and 2 are applied to the anesthetic-induced and organic solvent-induced enhancement of agonist binding to the nAChR. This response closely parallels anesthesia induced in tadpoles by the same compounds (12, 13) and therefore has special functional relevance. Possible mechanisms of enhancement of agonist binding have recently been discussed (18). The most probable mechanism is binding of the xenobiotic to a large number of noninteracting sites with an analogy of a "molecular lubricant" (18). We therefore examined whether the lipid/protein interface could provide this "lubricant."

The above equations were employed for a 1:1 stoichiometry of xenobiotic and lipid (q = 1) and the above two scenarios of the 1:3 stoichiometry (q = 3). The 1:3 stoichiometry was chosen in view of the size difference between lipid and xenobiotics. The analysis requires knowledge of the total number n of boundary lipid binding sites around the nAChR. This number is well known to be n = 40 on the basis of electron spin resonance spectroscopy (19). Next, the microscopic lipid binding constant derived from lipid activation curves (K_L) needs to be known. This constant had a rather uniform value of 3.75 ± 1.43 phospholipid molecules per protein molecule when lipid activation curves for Na+K+-ATPase, cytochrome oxidase, and sarcoplasmic reticulum Ca²⁺-ATPase were analyzed (15, 20). No precise phospholipid activation curves are available for the nAChR, but a highresolution activation curve for cholesterol has been published (21). Kinetic analysis of this curve by the regression procedure used for phospholipid activation (15, 20) confirmed a value of K_L = 3.75 lipid molecules per receptor molecule, the optimal number of tolerated vacant sites being a = 3 lipid molecules per receptor molecule. Cholesterol in this system thus behaved like a phospholipid activator. This result was consistent with the activation potential of a cholesterol-phospholipid hybrid (22) and with affinity labeling of the lipid/nAChR interface by a radioactive cholesterol analogue (23). In addition, a spin-labeled steroid derivative was found to occupy the same number of $n \sim 40$ binding sites that were occupied by spin-labeled phospholipid derivatives (19). The binding affinity of the steroid derivative to the nAChR was about 4-fold higher than that of the phospholipids (19).

The microscopic inhibitor dissociation constant K_I was determined by regression (least squares fit). For this purpose, the above Equations 1 and 2 were applied to published dose-effect curves for the enhancement of $[^3\mathrm{H}]$ acetylcholine binding by the anesthetic methoxyflurane and the organic solvents 1-hexanol, ether, and ethanol (12). The same type of kinetic analysis was performed on an independent data set for isoflurane and 1-butanol that caused enhanced binding of the fluorescent agonist molecule, $\mathrm{Dns-C_6-Cho}$ (13). The regression analysis was done using uniform concentration units of the number of lipid or xenobiotic molecules per nAChR molecule. The assumption of a 1:1 stoichiometry between lipid and xenobiotic allowed a good fit to the experimental data points, as shown together with the

Table I Results of the regression analysis

Calculated microscopic binding constants of xenobiotics K_I and derived free energies ΔG_b of the lipid relative to the binding of xenobiotic. The standard relationship given in the text was used for calculation of ΔG_b .

Compound	Sum of squared deviations for the various stoichiometries a				
	1:1	1:3 Scenario 1	1:3 Scenario 2	$K_I \cdot 10^{-4b}$	$\Delta G_b{}^c$
Ethanol	0.0875	0.0906	0.1724	23	-6.4
1-Butanol	0.0750	0.0536	0.0312	$(55)^{d}$	$(-6.9)^d$
1-Hexanol	0.0157	0.0165	0.0461	0.55	-4.2
Ether	0.0181	0.0186	0.1469	4.9	-5.5
Isoflurane	0.0183	0.0218	0.1332	1.4	-4.8
Methoxyflurane	0.0094	0.0100	0.0923	0.098	-3.2

- ^a Best fit given in bold face; the corresponding regression curves are depicted in Fig. 1.
- ^b Unit, number of xenobiotic molecules per receptor molecule.
- ^c Unit, kcal/mol, calculated for a temperature of 20 °C.
- ^d Value unreliable since based on the less favorable 1:1 stoichiometry.

regression curves for both scenarios of the 1:3 stoichiometry in Fig. 1. For comparison with the original data presentations (12, 13), relative activities are plotted *versus* log (molar xenobiotic concentration).

For five of the six xenobiotics discussed here, it can be seen from the curves of Fig. 1 and the data summarized in Table I that the first scenario of the 1:3 stoichiometry and the 1:1 stoichiometry yield very sound fits that are almost of the same quality and markedly better than the fit corresponding to the second scenario of the 1:3 stoichiometry. The fit derived from the 1:1 stoichiometry is a little better in each of these cases, but the difference in the sum of squared deviations is very small. This may be viewed as a robustness property of the underlying model. Different stoichiometries vield very similar results, which is important to know because 1:1 stoichiometry only was examined in Ref. 17. 1-Butanol behaves differently because the second scenario of the 1:3 stoichiometry yielded the best fit. The deviation was not due to a modeling artifact. Inspection of the experimental data indicates a definitely higher kinetic cooperativity of 1-butanol compared with the other xenobiotics.

The microscopic xenobiotic binding constants derived from the fitting procedure are summarized in Table I as are the sums of squared deviations. To estimate the free energy difference between the binding of lipid and xenobiotics, the standard equation $\Delta G_b = - \mathrm{RT} \, \ln(K_I/K_L)$ was applied to the K_I values of Table I using a constant K_L value of 3.75 lipid molecules per nAChR molecule. The ΔG_b values obtained for a uniform 1:1 stoichiometry are listed in Table I. As expected, the energetic difference between lipid and ethanol was greater than that between lipid and 1-hexanol. The energetic difference between ethanol and 1-hexanol amounted to -2.2 kcal/mol or -0.55 kcal/mol per methylene group. The latter value is close to the known transfer free energy value of -0.8 kcal/mol per methylene group (24).

The free energy value of -6.4 kcal/mol between ethanol and lipid may present the approximate free energy for the binding of membrane lipid to an integral membrane protein. It is generally not clear whether vacant lipid binding sites of membrane proteins are empty, occupied by water, or occupied by protein/ protein interaction. The reference to ethanol may provide an acceptable compromise for the uncertain standard state of an "empty" lipid binding site. A preliminary estimate of lipid/protein interaction energy has previously been derived from xenobiotic inhibition curves of the synaptosomal Ca²⁺-ATPase (15). The previous estimate of -7.1 kcal/mol (relative to chloroform) was similar to the present free energy value of -6.4 kcal/mol. Lipid/ protein interaction thus fulfills the common textbook definition (25) of a high energy bond. A recent review of helical membrane protein folding (26) thoroughly discusses lipid/protein interactions but contains no free energy estimates. In summary, the present analysis lends indirect support to the lipid/protein interface as the anesthetic target site and leads to the first available free energy estimate of lipid/protein interaction in membranes.

Acknowledgments—We thank Drs. K.W. Miller and D. Raines (Massachusetts General Hospital, Harvard Medical School, Department of Anesthesia and Critical Care) for stimulating discussions and for their permission to use the experimental data sets in Refs. 12 and 13.

APPENDIX

In this Appendix we derive the equations used under "Results and Discussion" from basic principles. The formulas may be used in a variety of scenarios, not just the one discussed in the present article. The mathematics may be considered elementary, but necessary equations (and the model assumptions underlying their derivation) are presented for the sake of clarity and for easy reference.

Several Ligands Occupying One Binding Site—We consider the following basic situation: A macromolecule P is equipped with n binding sites, and a ligand I may bind to any of these sites with a microscopic dissociation constant K_I . We assume that this constant is the same for each site and that binding is noncooperative in the classical sense. In contrast to the classical model, we allow that each site can be occupied by up to q ligands, with a fixed number q>0. Thus, the elementary reaction at one site in such a scenario is the binding of an I to a site not yet fully occupied, respectively the dissociation of an I from a site. The basic approach is similar to the previous discussion of the case q=1. (See Refs. 3, 15, 16, and 17.)

Numbering the sites from 1 to n, the state of P with some ligands bound to it is described by a tuple (d_1,\ldots,d_n) of nonnegative integers with d_j denoting the number of ligands at binding site j (thus d_j lies between 0 and q). We introduce the notations $P_{(d_1,\ldots,d_n)}$ to characterize a molecule of the corresponding binding status and $P_{(d_1,\ldots,d_n)}$ to denote the concentration of this type.

Mass action kinetics and microscopic reversibility lead to Equation 3,

$$P_{(d_1,\ldots,d_n)} + I \rightleftharpoons P_{(e_1,\ldots,e_n)}$$
 (Eq. 3)

and Equation 4.

$$p_{(d_1,\ldots,d_n)} \cdot y = p_{(e_1,\ldots,e_n)}$$
 (Eq. 4)

There is exactly one index k so that $e_k = d_k + 1$, and all other $e_i = d_i$. Here we have introduced the abbreviation $y = [I]/K_I$. From this basic description, a more convenient one is derived as follows.

To each state $P_{(d_1,\ldots,d_n)}$ one can associate another tuple $[s_0,\ldots,s_q]$ such that s_j denotes the number of binding sites holding exactly j ligands. Thus, all s_j are nonnegative and $s_0+\ldots+s_q=n$. By repeated application of Equation 4 it follows that $p_{(d_1,\ldots,d_n)}=p_{(e_1,\ldots,e_n)}$ whenever (d_1,\ldots,d_n) and

 (e_1,\ldots,e_n) give rise to the same tuple $[s_0,\ldots,s_q].$ Thus it is legitimate to introduce the state $P_{[s_0,\ldots,s_o]}$ and its concentration

 $\inf_{}^{p_{[s_0,\ldots,s_q]}}\inf_{}^{(d_{I},\ldots,d_n)}\text{ gives rise to }[s_0,\ldots,s_q]\text{, then the above remarks}$ imply the following Equation 5.

$$\binom{n}{s_1} \cdot \binom{n-s_1}{s_2} \cdot \cdot \cdot \binom{n-(s_1+\ldots+s_{q-1})}{s_q} \cdot p(d_1,\ldots,d_n) \quad \text{(Eq. 5)}$$

To verify this, note that there are $\binom{n}{s_1}$ possibilities for the sites with one ligand, after which there remain $\binom{n-s_1}{s_2}$ possibilities for the sites with two ligands, and so on. The natural ordering of the sequence $1,2,\ldots,q$ is of no importance here, since the formula also holds for any permutation of these integers.

Next, the counterpart of Equation 5 for the $p_{[s_0,\ldots,s_q]}$ will be derived. Adding one ligand to a state $P_{[s_0,\ldots,s_q]}$ changes it to a state $P_{[t_0,\ldots,t_q]}$ such that there is one index l>0 with $t_l=s_l+1$, $t_{l-1}=s_{l-1}-1$ and all other $t_j=s_j$. (Explanation: If one ligand is added to a site already occupied by l-1 ligands, there will be l ligands at this site afterward. Thus s_l increases by one, and s_{l-1} decreases by one.) Using Equations 4 and 5, and a permutation of 1,2,...,q that has l in the first position and l-1 in the second, we find the following,

$$\binom{n}{s_l+1} \binom{n-(s_l+1)}{s_{l-1}-1} \cdot F \cdot p_{[s_0,\ldots,s_q]} \cdot y$$

$$= \binom{n}{s_l} \binom{n-s_l}{s_{l-1}} \cdot F \cdot p_{[s_0,\ldots,t_q]} \quad (\text{Eq. 6})$$

where we have abbreviated F for a product of terms that appear on both sides of the equation. Cancellation of terms leads to Equation 7.

$$\frac{s_{l-1}}{s_l+1} \cdot p_{[s_0,\ldots,s_q]} \cdot y = p_{[t_0,\ldots,t_q]}$$
 (Eq. 7)

Here the positive integer l is distinguished by the property that a ligand is added to a site occupied by l-1 ligands. For q=1 we obtain the standard result (27), as should be expected.

Formulas and Recursions-We derive a number of closedform expressions for the concentration terms. The fundamental formula is the following one for the $p_{[s_0,\ldots,s_q]}$, where for reasons of convenience one sets in Equation 8,

$$s_0 = n - r_0, s_1 = r_0 - r_1, \dots, s_{q-1} = r_{q-2} - r_{q-1}, s_q = r_{q-1},$$
 (Eq. 8)

with $n \ge r_0 \ge r_1 \ge \ldots \ge r_q - l$ and Equation 9 results.

 $p_{[n-r_0,r_0-r_1,\ldots,r_{q-2}-r_{q-1},r_{q-1}]}$

$$= \binom{n}{r_0} \cdot \binom{r_0}{r_1} \cdots \binom{r_{q-2}}{r_{q-1}} \cdot y^{r_0 + \ldots + r_{q-1}} \cdot p_{[n,0,\ldots,0]} \quad \text{(Eq. 9)}$$

Here $p^* = p_{[n,0,\ldots,0]}$ is the concentration of macromolecules with no ligand attached. (To prove this formula, use Equation 7 and mathematical induction.)

Next we present closed expressions for sums of certain concentration terms. (Since the proofs are elementary from a mathematician's perspective, and of little interest for nonmathematicians, they are omitted.) The total concentration of those molecules where exactly d (with $0 \le d \le n$) sites are filled with q ligands is given by the expression shown in Equation 10.

$$\sum_{r_0,\ldots,r_{q-2}} p_{[n-r_0,r_0-r_1,\ldots,r_{q-2}-d,d]}$$

$$= \binom{n}{d} \cdot y^{qd} \cdot (1 + y + \ldots + y^{q-1})^{n-d} \cdot p^* \quad \text{(Eq. 10)}$$

Here the summation extends over all tuples $(r_0,\ldots,r_q-{}_2)$ such that $d \leq r_q - 2 \leq \ldots \leq r_0 \leq n$.

The total concentration of molecules in states where exactly n-d sites contain no ligands is given by the expression shown in Equation 11.

$$\sum_{r_1, \dots, r_{q-1}} p_{[n-d, d-r_1, \dots, r_{q-2}-r_{q-1}, r_{q-1}]} = \binom{n}{d} \cdot (y + \dots + y^q)^d \cdot p^*$$
 (Eq. 11)

Here the summation extends over all tuples $(r_1, ..., r_q - l)$ such

that $d \ge r_1 \ge \ldots \ge r_{q-2} \ge r_{q-1}$.

Two Types of Ligands (First Scenario)—Now we introduce another ligand, denoted L, that binds to the sites of P with a dissociation constant K_L . The standard assumption that only one L may bind at each site leads to two types of elementary reactions: First, binding of I to a site not yet fully occupied, or dissociation of I from an occupied site. Second, binding of L to a site where this is still possible, or dissociation of L from an occupied site. Moreover, it is assumed that L may still bind to a site already occupied by ligands I, provided that there are fewer than q ligands I at this particular site. (In other words, only sites completely filled with I are inaccessible for L.) Therefore, the states are described by classes $P_{1,[n-r_0,r_0-r_1,\ldots,r_{q-l}]}$ (with concentrations $p_{1,[n-r_0,r_0-r_1,\ldots,r_{q-l}]}$, where the tuple $[n\text{-}r_0,\ r_0-r_1,\ldots l]$ describes the binding state of ligands I, whereas the integer l, $0 \le l \le n - r_{q-1}$, denotes the number of bound ligands L. Denoting $x = [L]/K_L$, mass action law and microscopic reversibility yield Equation 12.

$$\frac{n-r_{q-1}-l}{l+1} \cdot p_{l,[n-r_0,r_0-r_1,\dots]} \cdot x = p_{l+1,[n-r_0,r_0-r_1,\dots]} \tag{Eq. 12}$$

(Note that this is a special case of Equation 7 for L, with q = 1.) Therefore, Equation 13,

$$p_{l,[n-r_0,r_0-r_1,\ldots,d]} = \binom{n-d}{l} \cdot p_{0,[n-r_0,r_0-r_1,\ldots,d]} \cdot x^l$$
 (Eq. 13)

follows by induction, and using Equation 9, we have Equation

$$\sum_{r_0,\ldots,r_{q-2}} p_{l,[n-r_0,r_0-r_1,\ldots,r_{q-2}-d,d]} = \binom{n}{d} \cdot \binom{n-d}{l}$$

$$\cdot x^l \cdot y^{qd} \cdot (1 + y + \ldots + y^{q-1})^{n-d} \cdot p^*$$
 (Eq. 14)

(Here l and d are fixed, and summation extends over those r_0, \ldots, r_{q-2} with $n \ge r_0 \ge \ldots \ge r_{q-2} \ge d$.) Moreover Equation 15

$$\sum_{l=0}^{n-d} \sum_{r_0,\ldots,r_{q-2}} p_{l,[n-r_0,r_0-r_1,\ldots,r_{q-2}-d,d]} = \binom{n}{d} \cdot (1+x)^{n-d} \cdot y^{qd}$$

$$\cdot (1 + y + \ldots + y^{q-1})^{n-d} \cdot p^*$$
 (Eq. 15)

and the total concentration is equal to the following, shown in Equation 16.

$$\sum_{d=0}^{n} \sum_{l=0}^{n-d} \sum_{r_0, \dots, r_{r-2}} p_{l, [n-r_0, r_0-r_1, \dots, r_{q-2}-d, d]}$$

=
$$((1+x)\cdot(1+y+\ldots+y^{q-1})+y^q)^n\cdot p^*$$
 (Eq. 16)

In the model under consideration in this paper, there is a positive integer a so that only the molecules with n-a or more ligands L are active (and hence of interest). Their total concentration can be found from the above as shown in Equation 17.

$$\sum_{d=0}^{a}\sum_{l=n-a}^{n-d}\binom{n}{d}\cdot\binom{n-d}{l}\cdot x^l\cdot y^{qd}\cdot (1+y+\ldots+y^{q-1})^{n-d}\cdot p^* \qquad \text{(Eq. 17)}$$

To summarize, the relative proportion of the active molecules is given by Equation 18.

$$r = \frac{\sum_{d=0}^{a} \binom{n}{d} \cdot y^{qd} \cdot (1 + y + \dots + y^{q-1})^{n-d} \cdot \sum_{l=n-a}^{n-d} \binom{n-d}{l} \cdot x^{l}}{((1+x)(1+y+\dots+y^{q-1}) + y^{q})^{n}}$$
(Eq. 18)

This is Equation 1 from "Results and Discussion."

Two Types of Ligands (Second Scenario)—We start as in A.3, but now the basic assumption is that only vacant sites can be occupied by L. Again we characterize molecule binding states by classes $P_{1,[n-r_0,r_0-r_1,\ldots,r_{q-1}]}$ (with concentrations $p_{1,[n-r_0,r_0-r_1,\ldots,r_{q-1}]}$), but in this situation one has $0 \le l \le n-r_0$. Similar to Equation 13, one derives Equation 19,

$$p_{l,[n-d,d-r_1,\ldots,r_{q-1}]} = \binom{n-d}{l} \cdot p_{0,[n-d,d-r_1,\ldots,r_{q-1}]} \cdot x^l \qquad \text{(Eq. 19)}$$

and with the help of Equation 11, one gets Equation 20.

$$\sum_{r_{1,...,r_{q-1}}} p_{l,[n-d,d-r_{1,...,r_{q-1}}]} = \binom{n}{d} \cdot \binom{n-d}{l} \cdot x^{l} \cdot (y+...+y^{q})^{d} \cdot p^{*} \quad (\text{Eq. 20})$$

The total concentration is equal to the following, shown in

$$\sum_{d} \sum_{l} \sum_{r_1, \dots, r_{q-1}} p_{l, [n-d, d-r_1, \dots, r_{q-1}]} = (1 + x + y + \dots + y^q)^n \cdot p^*$$
 (Eq. 21)

The relative proportion of active molecules here equals the following, derived in Equation 22.

$$r = \frac{\sum_{d=0}^{a} \binom{n}{d} \cdot (y + \dots + y^q)^d \cdot \sum_{l=n-a}^{n-d} \binom{n-d}{l} \cdot x^l}{(1 + x + y + \dots + y^q)^n}$$
 (Eq. 22)

This is Equation 2 from "Results and Discussion." As is expected, in the case q = 1, this is the same result as the one provided by Equation 18.

REFERENCES

- 1. Franks, N. P., and Lieb, W. R. (1998) Toxicol. Lett. (Amst.) 100-101,1-8
- 2. Sandberg, W. S., Dubois, B. W., and Miller, K. W. (1999) Curr. Top. Membr. 48,
- 3. Sandermann, H. (1982) Eur. J. Biochem. 127, 123-128
- 4. Sandermann, H., Duncan, T. M., McIntyre, J. O., and Fleischer, S. (1993) in Protein-Lipid Interactions (Watts, A., ed), pp. 67-85, Elsevier, Amsterdam
- Sandermann, H. (1984) FEBS Lett. 168, 271-274
- 6. Sandermann, H., McIntyre, J. O., and Fleischer, S. (1986) J. Biol. Chem. 261,
- 7. Loeb-Hennard, C., and McIntyre, J. O. (2000) Biochemistry 39, 11928-11938
- 8. Hannun, Y. A., and Bell, R. M. (1990) J. Biol. Chem. 265, 2962–2972 9. Newton, A, C., and Koshland, D. E. (1989) J. Biol. Chem. 264, 14909-14915
- 10. Sandermann, H., and Duncan, T. M. (1991) Biochim. Biophys. Acta 1069,
- 235 240
- 11. Mosior, M., and Newton, A. C. (1998) Biochemistry 37, 17271-17279 12. Miller, K. W., Braswell, L. M., Firestone, L. L., Dodson, B. A., and Forman,
- S. A. (1986) in Molecular and Cellular Mechanisms of Anaesthetics (Roth, S. H., and Miller, K. W., eds), pp. 125-137, Plenum Medical Book Company,
- 13. Raines, D. E., Rankin, S. E., and Miller, K. W. (1995) Anesthesiology 82, 276 - 287
- 14. Popot, J.-L., Demel, R. A., Sobel, A., van Deenen, L. M., and Changeux, J.-P. (1978) Eur. J. Biochem. 85, 27-42
- 15. Pflugmacher, D., and Sandermann, H. (1998) Biochim. Biophys. Acta 1415, 174 - 180
- 16. Sandermann, H. (1993) Biochim. Biophys. Acta 1150, 130-133
- 17. Sandermann, H., and Pflugmacher, D. (1996) Biochim. Biophys. Acta 1300, 219 - 225
- 18. Miller, K. W., Addona, G. H., and Kloczewiak, M. A. (1998) Toxicol. Lett. (Amst.) 100-101,139-147
- 19. Ellena, J. F., Blazing, M. A., and McNamee, M. G. (1983) Biochemistry 22, 5523-5535
- 20. Kliem, D. (1999) Die Lipid/Protein-Grenzfläche von Membranenzymen als Angriffsort von Anästhetika, Ph.D. dissertation, Ludwig-Maximilians-Universität München
- 21. Rankin, S. E., Addona, G. H., Kloczewiak, M. A., Bugge, B., and Miller, K. W. (1997) Biophys. J. 73, 2446-2455
- 22. Addona, G. H., Sandermann, H., Kloczewiak, M. A., Husain, S. S., and Miller, K. W. (1998) Biochim. Biophys. Acta 1370, 299–309
- 23. Corbin, J., Wang, H. H., and Blanton, M. P. (1998) Biochim. Biophys. Acta **1414.** 64-74
- Gennis, R. B. (1989) Biomembranes Molecular Structure and Function, pp. 56-57, p. 266, Springer-Verlag, New York
- 25. Stryer, L. (1975) Biochemistry, W. H. Freeman, San Francisco
- 26. Popot, J.-L., and Engelman, D. M. (2000) Annu. Rev. Biochem. 69, 881-922
- 27. Segel, L. A. (1991) Biological Kinetics, Cambridge University Press,

The Lipid/Protein Interface as Xenobiotic Target Site: KINETIC ANALYSIS OF THE NICOTINIC ACETYLCHOLINE RECEPTOR

Sebastian Walcher, Joachim Altschuh and Heinrich Sandermann, Jr.

J. Biol. Chem. 2001, 276:42191-42195. doi: 10.1074/jbc.M105136200 originally published online August 6, 2001

Access the most updated version of this article at doi: 10.1074/jbc.M105136200

Alerts:

- When this article is cited
- When a correction for this article is posted

Click here to choose from all of JBC's e-mail alerts

This article cites 19 references, 3 of which can be accessed free at http://www.jbc.org/content/276/45/42191.full.html#ref-list-1